European Polymer Journal 47 (2011) 1081–1089

Contents lists available at ScienceDirect

European Polymer Journal

journal homepage: www.elsevier.com/locate/europolj

Novel DOPO-based flame retardants in high-performance carbon fibre epoxy composites for aviation

B. Perret [a], B. Schartel [a,*], K. Stöß [b], M. Ciesielski [b], J. Diederichs [b], M. Döring [b], J. Krämer [c], V. Altstädt [c]

[a] BAM Federal Institute for Materials Research and Testing, Unter den Eichen 87, D-12205 Berlin, Germany
[b] Institute of Technical Chemistry, KIT Karlsruhe Institute of Technology, Hermann-von-Helmholtz-Platz 1, D-76344 Eggenstein-Leopoldshafen, Germany
[c] Department of Polymer Engineering, University of Bayreuth, Universitätsstraße 30, D-95447 Bayreuth, Germany

ARTICLE INFO

Article history:
Received 10 November 2010
Received in revised form 31 January 2011
Accepted 10 February 2011
Available online 16 February 2011

Keywords:
Epoxy resin (RTM6)
DOPO
Carbon fibre reinforced composites
Mechanical properties
Flame retardancy

ABSTRACT

Two novel, halogen-free, phosphorus-based oligomeric flame retardants are investigated in the commercial epoxy resin RTM6 and ~70 wt.% carbon fibre RTM6 composites (RTM6-CF) with respect to pyrolysis and fire behaviour. The flame retardants are based on 9,10-dihydro-9-oxy-10-phosphaphenanthrene-10-oxide (DOPO) units linked to the star-shaped aliphatic ground body tetra-[(acryloyloxy)ethyl] pentarythrit (DOPP), or heterocyclic tris-[(acryloyloxy)ethyl] isocyanurate (DOPI), respectively. The glass transition temperature is reduced by adding DOPP and DOPI, but the mechanical properties of the composites (e.g. interlaminar shear strength (ILSS) and G_c in mode I and II) remain unchanged. Decomposition models are proposed based on mass loss, evolved gas analysis (TG–FTIR) and condensed product analysis (hot stage cell within FTIR). The fire behaviour is investigated comprehensively (UL 94, limiting oxygen index (LOI) and cone calorimeter). Both flame retardants act in the gas phase through flame inhibition and in the condensed phase through charring. The UL 94 of RTM6 is improved from HB to V-1 and V-0; the LOI from 25% to 34–38%. Peak heat release rate (PHRR) and total heat evolved (THE) are lowered by 31-49% and 40–44%, respectively. Adding CF increases the residue, reduces the THE, but suppresses the charring due to RTM6 and flame retardants. Thus the THE of RTM6-CF is reduced by about 25% when DOPI and DOPP are added. However, UL 94: V-0 and LOI of 45% and 48% are achieved with ~0.6 wt.% phosphorus.

1. Introduction

Epoxy resins display excellent properties such as high thermal and mechanical stability and good chemical resistance [1,2]. Reinforced with carbon fibres (CF), their composites are used increasingly in applications where conventional materials, such as metals, are too costly due to their high weight. Composites stand out due to their low weight, improved mechanical properties and absence of corrosion [3]. They have already replaced several aluminium parts in airplanes in civil and military aviation. Unfortunately, epoxy resins perform very poorly in a fire, since most of them burn easily and violently [3]. Especially in the transportation sector, fire-protection requirements have to be fulfilled, making the flame retardancy of epoxy resins and their composites an important issue [4]. Flame retardants containing phosphorus seem to offer a promising halogen-free way to render epoxy resins and their composites flame retardant in the future [5,6]. Thus 9,10-dihydro-9-oxa-10-phosphaphenanthrene-10-oxide (DOPO) has become one of the most important flame retardants in this field, now used in several modifications as a reactive or additive compound [7–14]. DOPO shows excellent flame-retarding properties in epoxy-based materials. Thereby DOPO can either act only in the gas phase via flame inhibition, or in the gas phase and in the condensed phase (via char formation) at the same time [10,11,15].

* Corresponding author. Tel.: +49 30 8104 1021; fax: +49 30 8104 1617.
E-mail address: bernhard.schartel@bam.de (B. Schartel).

0014-3057/$ - see front matter © 2011 Elsevier Ltd. All rights reserved.
doi:10.1016/j.eurpolymj.2011.02.008

However, it is often observed that adding DOPO-compounds, in particular, or incorporating them reactively into the epoxy network, lowers the glass transition temperature and has negative effects on the mechanical properties. It is proposed that oligomeric and polymeric DOPO-compounds with high molecular weight diminish these drawbacks. Further it seems that the molecular structure of the additives plays an important role [16]. Thus in this paper we present two new oligomeric star-shaped DOPO-based flame retardants, DOPP and DOPI (Fig. 1), both bearing four and three DOPO moieties, respectively, linked to a ground body. The ground body of DOPP consists of tetra-[(acryloyloxy)ethyl] pentarythrit; that of DOPI is made of tris-[(acryloyloxy)] ethyl isocyanurate. The epoxy system used was the commercial monocomponent system RTM6, which mainly consists of tetraglycidyl methylendianiline as epoxy and methylene-bis-(2,6-diethylaniline) and methylene-bis-(2,6-diisopropylaniline) as aromatic hardeners. RTM6 is widely used in aviation industry due to its high toughness and its high glass transition temperature.

The focus of this study lies on the influence of the two flame retardants on the glass transition temperature and mechanical properties, on the thermal decomposition and on the fire behaviour of the thermosets and composites. With the results on mass loss, evolved gas and condensed product analysis, decomposition mechanisms were proposed. The flammability (reaction to a small flame) and the fire behaviour was determined and compared with CF reinforced equivalents.

2. Experimental

2.1. Synthesis of the flame retardants

DOPP (Fig. 1a): toluene (1200 ml) was placed in a 4-l four-necked round bottom flask equipped with a stirrer, a thermometer and a condenser. The solvent was heated to 373 K and 1800 g (8.33 mol) DOPO (Schill + Seilacher GmbH) was added slowly while stirring. When DOPO was dissolved completely, triethylamine (115 ml; 84 g; 0.83 mol) was added. Then a mixture of tetra-[(acryloyloxy)ethyl] pentarythrit (810 g, 2.30 mol, Sartomer, used as received) and toluene (180 ml) was fed into the reaction mixture via the dropping funnel over 3 h such that the temperature did not exceed 378 K. After the mixture was stirred for a further 2 h at 373 K, a sample was taken and analysed by means of ^{1}H nuclear magnetic resonance spectroscopy (NMR). If a portion of one reactant remained unreacted, the required amount of the other was added. Then the mixture was stirred for a further 2 h. Next the main part of the solvent was distilled off. The obtained viscous substance was gradually heated up to 473 K, whereby the pressure was gradually decreased to 10 mbar. The melt was maintained at 473 K and 10 mbar for 6 h, then poured into a steel bowl and cooled to room temperature. The obtained glassy solid was crushed and milled to yield the DOPP as a white powder. The synthesised flame retardants were characterised with ^{1}H- and ^{31}P-NMR (Bruker AC-250) using tetramethylsilane and trimethylphosphate as internal standards. Spin multiplicity is indicated: (broad) singlet, duplet, triplet, quartet and multiplet. ^{1}H-NMR ($CDCl_3$): δ = 2.20–2.38 (m, 8H), 2.48–2.67 (m, 8H), 3.90–4.08 (bs, 8H), 7.12–7.23 (m, 8H), 7.26–7.36 (m, 4H), 7.40–7.52 (m, 4H) 7.58–7.69 (m, 4H), 7.76–7.95 (m, 12H) ppm; ^{13}C-NMR ($CDCl_3$): δ = 22.65, 24.22, 26.26, 41.82, 62.08, 120.13, 120.22, 121,72, 121,90, 122,44, 123,80, 123.94, 124,37, 124.69, 125.10, 128.37, 128.57, 129.76, 129.93, 130.57, 133.44, 135.37, 135.47, 148.55, 148.69, 170.87, 171.13 ppm; ^{31}P-NMR ($CDCl_3$): δ = 37.4 ppm. A Voyager System 6059 from Applied Biosystems was used to perform MALDI–TOF mass spectrometry using 2,6-dihydroxyacetophenon as matrix. $m/z = (M^+)$, 1217.4 ($C_{65}H_{56}P_4O_{16}$) (1217.03): elemental analysis was carried out using a Vario EL III from Elementar Analysensysteme GmbH. Calculated: C 64.15 wt.%, H 4.64 wt.%, O 21.03 wt.%, P 10.18 wt.%;

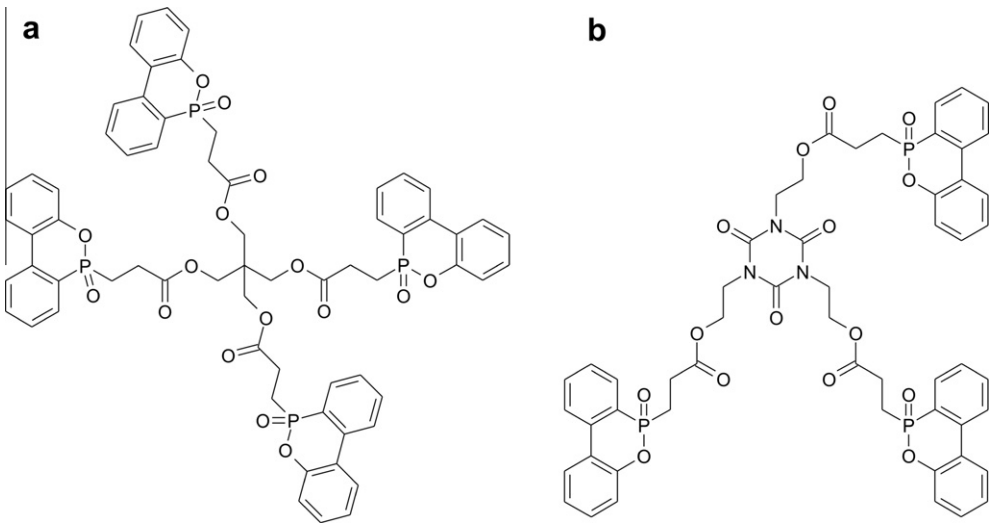

Fig. 1. Structures of the flame retardants (a) DOPP and (b) DOPI.

Found: C 63.70 wt.%, H 4.83 wt.%. The synthesis of DOPI (Fig. 1b) has been described in an earlier paper [17]. DOPI: $C_{54}H_{48}N_3P_3O_{15}$, calculated: C 60.51 wt.%, H 4.51 wt.%, N 3.93 wt.%, O 22.39 wt.%, P 8.67 wt.%.

2.2. Preparation of the samples

The composition of the different materials is presented in Table 1. All thermosets contained 2 wt.% and the corresponding CF composites around 0.6 wt.% of phosphorus. The final products were prepared according to the following experimental procedure. The RTM6 was placed in a glass flask and heated to 393 K in an oil bath. The desired amounts of DOPP and DOPI, respectively, were added and mixed extensively for 45 min until complete dissolution. The mixtures were degassed for 5–10 min in a vacuum mixer at 393 K and then cured in an aluminium mould in a convection oven to obtain compact plaques. The curing cycle was 2 K min^{-1} from 393 to 453 K and held at 453 K for 2 h. Then curing was completed with a -2 K min^{-1} ramp from 453 K down to room temperature. RTM6 without flame retardant was cured following an identical procedure. All ~70 wt.% CF-reinforced composites were manufactured by vacuum-assisted resin transfer molding (VARTM). The feasibility for this procedure was proven by viscosity measurements [18]. The fibres were arranged in a perpendicular alignment. The mould was preconditioned with a release agent (Loctite 770-NC Frekote), evacuated and heated up to 393 K prior to impregnation of the dry fabrics with the epoxy resin, applying a pressure of 1.5 bar. After complete impregnation, a dwell pressure of 2.5 bar was applied for 10 min. The (post-) curing cycles were identical to the thermosets.

2.3. Characterisation of the glass transition temperature, mechanical properties, pyrolysis and fire behaviour

Dynamic mechanical analysis (DMA) was performed using a RDAIII from Rheometric Scientific at a heating rate of 3 K min^{-1} from 298 to 573 K. The rectangular specimens of 50 × 10 × 2 mm cut out of the cured plates were used in the torsion rectangular geometry mode, at a frequency of 3 Hz and 0.1% deformation. The glass transition temperature (T_g (3 Hz)) was determined using the maximum of tan δ. According to the DIN EN 2563 specification, interlaminar shear strength (ILSS) tests (short beam) were performed. Rectangular specimens (25 × 10 × 3 mm) were tested using a Zwick Z050 operating at a constant cross-head displacement speed of 1 mm min^{-1} at room temperature. The maximum apparent shear strength in the mid-plane of the composite was approximated by the Euler–Bernoulli beam theory. The interlaminar energy release rates in mode I and mode II (G_{Ic}, G_{IIc}) were measured following DIN 65 563. Five samples (250 × 25 × 3 mm) were tested using a Zwick Z2.5 at a constant cross-head displacement speed of 10 mm min^{-1} for the G_{Ic} and 1 mm min^{-1} for the G_{IIc} test, respectively, at room temperature.

Table 1
Investigated materials.

	Epoxy resin/wt.%	Flame retardant/wt.%	Carbon fibres/wt.%
RTM6	100	–	–
RTM6-CF	30.5	–	69.5
RTM6 + DOPP	80.4	19.6	–
RTM6-CF + DOPP	24.2	5.9	69.9
RTM6 + DOPI	76.9	23.1	–
RTM6-CF + DOPI	23.1	6.9	70.0

The thermal decomposition of the non-reinforced materials was investigated by thermogravimetry using a TGA/SDTA 851 (Mettler Toledo, Germany). Evolved gas-phase analysis was carried out by coupling a heated gas analysis cell (533 K) of a Fourier transform infrared spectrometer (FTIR, Nexus 470, Nicolet, Germany) with the thermogravimetry using a heated (523 K) transfer line. The experiments were performed with a sample mass of 5 mg at a heating rate of 10 K min^{-1} under nitrogen. Thermal decomposition in the condensed phase of the non-reinforced materials was analysed using a Linkam FTIR hot stage cell (Linkam, UK) within the FTIR. RTM6 was heated up to 353 K and then DOPP and DOPI, respectively, were added with a phosphorus concentration of 2 wt.%. The mixture was stirred at 353 K for 5 min, exposed to a KBr target as thin film, and then immediately placed in the vertically mounted FTIR hot stage cell. The films were heated from 303 K up to 873 K at a heating rate of 10 K min^{-1} in a nitrogen atmosphere.

The forced-flaming behaviour of the thermosets and the CF composites was investigated using a cone calorimeter (FTT, UK) following ISO 5660 (irradiation = 50 kW m^{-2}). The samples (100 × 100 × 3 mm) were wrapped in aluminium foil and placed horizontally under the cone heater at a distance of 35 mm. Flammability (reaction to a small flame) was investigated by the limiting oxygen index (LOI) following ISO 4589 and by UL 94 vertical (V2, V1, V0) and horizontal (HB) classifications following IEC 60695-11-10. The sample size for the LOI was 150 × 7 × 3 mm; that for the UL 94 test was 125 × 12.5 × 3 mm.

3. Results and discussion

3.1. Glass transition temperature and mechanical properties

The glass transition temperatures of the investigated materials, T_g (3 Hz), are summarised in Table 2. The T_g decreased significantly (between 14 and 54 K) when 19.6 wt.% DOPP, 23.1 wt.% DOPI or approximately 70 wt.% CF were added to RTM6. The decrease in T_g is attributed to a reduction in the effective number of cross-linking points per volume, due mainly to the modification of replacing epoxy resin with the flame retardant [9]. The drop of the T_g for RTM6 + DOPI and RTM6-CF + DOPI (T_g = 449 and 448 K) is critical, since a T_g of at least 453 K is usually required for aircraft exploitation. However, in the case of RTM6 + DOPP and RTM6-CF + DOPP (T_g = 464 and 463 K) the T_g is kept on a high performance level. The reduction in the composites in comparison to the corresponding thermosets may be due at least in part to the finishing of the CF.

The composites were free of delamination and porosity, indicated by ultrasonic scans [18]. The flame-retarded

Table 2
Glass transition temperatures T_g (3 Hz), apparent interlaminar shear strength (ILSS) and critical energy release rate (mode I: G_{Ic}; mode II: G_{IIc}) of the composites.

	T_g/K	ILSS/M Pa	G_{Ic}/J m^{-2}	G_{IIc}/J m^{-2}
RTM6	502 ± 2	–	–	–
RTM6 + DOPP	464 ± 2	–	–	–
RTM6 + DOPI	449 ± 2	–	–	–
RTM6-CF	488 ± 2	67 ± 2	353 ± 17	1066 ± 36
RTM6-CF + DOPP	463 ± 2	61 ± 3	356 ± 49	1075 ± 160
RTM6-CF + DOPI	448 ± 2	62 ± 4	335 ± 44	1183 ± 220

composites showed ILSS values very similar to RTM6-CF, albeit slightly lower (Table 2). This slight reduction is due mainly to decreased fibre matrix adhesion [19] as a consequence of the high amount of additives. The critical strain energy release rate (G_c) was not affected significantly. Both the G_{Ic} and the G_{IIc} of RTM6-CF + DOPP and RTM6-CF+ DOPI were in the margin of error compared to those of RTM6-CF. Thus the oligomeric star-shaped flame retardants used do not worsen the mechanical properties such as apparent interlaminar shear strength and critical strain energy release.

3.2. Pyrolysis: mass loss

Thermogravimetry results of DOPP, DOPI, RTM6, RTM6 + DOPP and RTM6 + DOPI are shown in Fig. 2 and Table 3. DOPP decomposed in a single decomposition step with a maximum mass loss rate (T_{max}) at 725 K and around 10 wt.% residue. DOPI showed two decomposition steps with T_{max} at 708 and 726 K, respectively, and left around 11 wt.% residue. RTM6 decomposed in a single decomposition step with a T_{max} at 673 K and a residue of around 8 wt.%. RTM6 + DOPP and RTM6 + DOPI also decomposed in a single step; the T_{max} for both was close to that of RTM6. No additional decomposition step was observed due to the flame retardants at higher temperatures.

The residue for RTM6 + DOPP was around 18 wt.% and that for RTM6 + DOPI around 17 wt.%. Thus both residues were much higher than the residues calculated on the basis of superimposing the residues of the individual materials (RTM6, DOPP and DOPI) (Table 3). Both flame retardants work in the condensed phase by enhancing the char formation.

3.3. Pyrolysis: evolved gas analysis

The TG–FTIR analysis of the volatile pyrolysis gases of RTM6 + DOPP showed a release of low-molecular weight products, such as water and carbonyls with characteristic absorption bands at 3905 and 1731 cm^{-1}, respectively. Further, primary aniline compounds (3499 cm^{-1}) with aliphatic moieties from side chains of the aniline derivatives (2969, 2937 and 2885 cm^{-2}) and methane (1305, 3015 cm^{-1}) were released. Compounds containing phosphorus, such as P═O at 1233 cm^{-1}, P—O—C_{Ar} at 1118 and 1475 cm^{-1} and P—C_{Ar} at 1431 cm^{-1} were observed as well, indicating the thermal decomposition of DOPP. Adding DOPI to RTM6 did not change the kind of decomposition products in comparison to RTM6 + DOPP, apart from an additional absorption band at 1818 cm^{-1} indicating oxazolidinone derivatives. The release of carbonyl compounds was lowered. The same phosphorus absorption bands were observed.

The product release rates of DOPP and DOPI are shown in Fig. 3. The thermal decomposition of RTM6 + DOPP started with the release of water and carbonyls, reflecting a dehydratisation and carbonyl splitting from the 2-hydroxytrimethylene groups of the epoxy matrix, in good agreement with results reported in the literature [20–22]. The thermal decomposition of RTM6 + DOPI started with the release of water and oxazolidinone, while carbonyl compounds vanished almost completely. Oxazolidinone indicates an early decomposition of the isocyanurate ring of the flame retardant. Subsequently primary aniline compounds with aliphatic side chains evolved in both RTM6 + DOPP and RTM6 + DOPI, indicating decomposition of the epoxy backbone. Methane was released in a two-stage process, while the main release at the end of the decomposition represents the polyaromatisation of the char. The maximum of the product release rates of water, primary anilines and methane is nearly equal in both materials. The release of phosphorus compounds was ob-

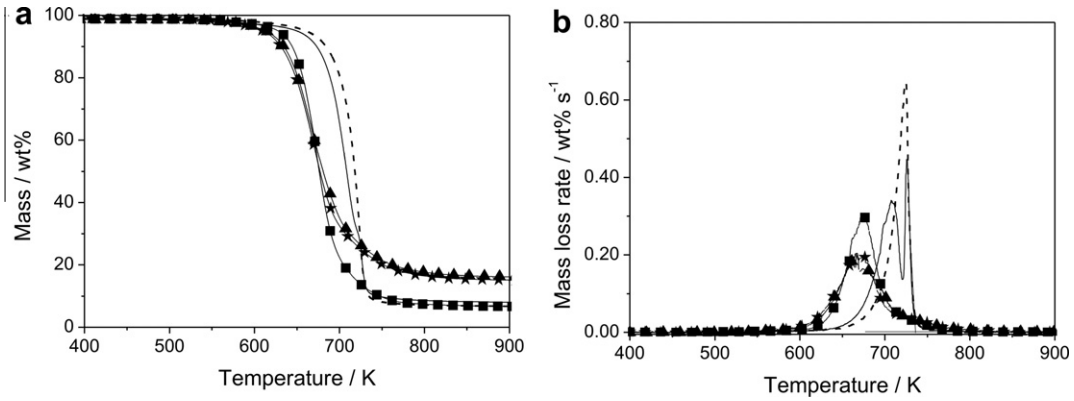

Fig. 2. (a) Mass and (b) mass loss rate of DOPP (dashed line), DOPI (solid line), RTM6 (filled squares), RTM6 + DOPP (filled triangles) and RTM6 + DOPI (filled stars).

Table 3
Thermal analysis of RTM6, DOPP, DOPI, RTM6 + DOPP and RTM6 + DOPI.

	DOPP	DOPI	RTM6	RTM6 + DOPP	RTM6 + DOPI
T_2wt%/K ± 2	560	565	572	560	565
T_{max}/K ± 2	725	708/726	673	667	667
Mass loss/wt.% ± 1	90.2	88.6	91.5	81.8	83.1
Residue/wt.% ± 1	9.8	11.4	7.8	18.2	17.3
Calc. residue/wt.% ± 1	–	–	–	8.8	9.2

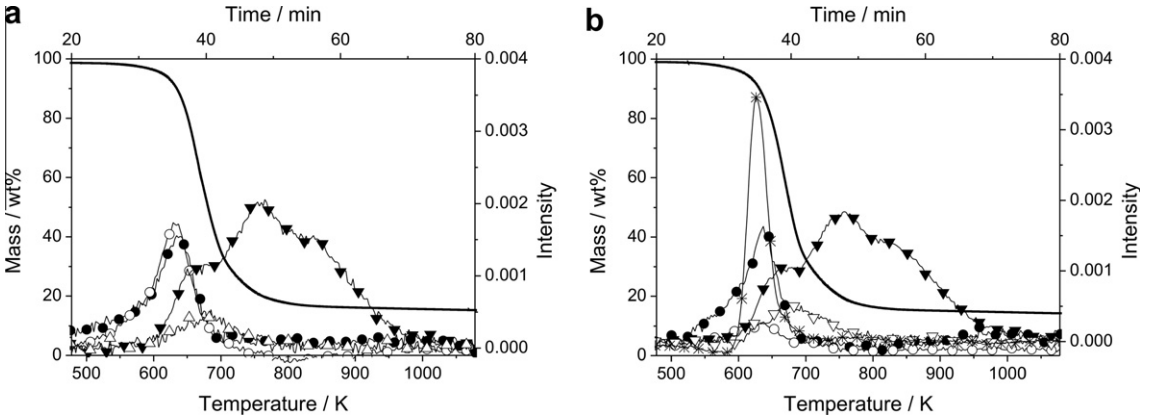

Fig. 3. Mass (solid lines) and product release rates of (a) RTM6 + DOPP and (b) RTM6 + DOPI (filled circles = water (3905 cm^{-1}), open circles = carbonyls (1731 cm^{-1}), filled inverted triangles = methane (3015 cm^{-1}), open inverted triangles = primary aniline derivatives (3499 cm^{-1}), crosses = oxazolidinone (1818 cm^{-1})).

served at the main decomposition step in both RTM6 + DOPP and RTM6 + DOPI.

3.4. Pyrolysis: condensed-product analysis

FTIR spectra of the condensed phase of RTM6 + DOPP and RTM6 + DOPI at different stages of thermal decomposition are shown in Fig. 4. The spectra of both materials did not differ significantly from each other. Before curing at 300 K the spectra showed absorption bands of amines and aromatic rings originating from the epoxide and the hardener (3465 and 3390 cm^{-1} N—H stretching vibration of primary amines; 1233 and 1190 cm^{-1} C—N stretching vibration, 1614 and 1517 cm^{-1} C—C stretching vibration of aromatic ring). The epoxy group yielded stretching vibrations at 1260 and 907 cm^{-1}. The flame retardants showed absorption bands at 1742 cm^{-1} (C═O stretching vibration of ester group), 1475 and 1118 cm^{-1} (P—O—C_{Ar} stretching vibration) and 754 cm^{-1} (C_{Ar}—H deformation of ortho-substituted aromatic ring). RTM6 + DOPI additionally showed a C—N stretching vibration of the isocyanurate ring at 1697 cm^{-1}.

The spectra changed significantly with increasing temperature. While some absorption bands disappeared, new absorption bands were formed. At 500 K the band of the epoxy groups at 1260 cm^{-1} vanished completely and the band at 907 cm^{-1} broadened and shifted to higher wavenumbers (to 911 cm^{-1}), uncovering a P—O—C_{Ar} stretching vibration of phosphorus which was overlapped by the epoxy band. New absorption bands of secondary hydroxy groups appeared at 3566 (O—H stretching) and 1043 cm^{-1} (O—H deformation) monitoring the curing process of the epoxy resin. At the end of thermal decomposition these bands vanished completely, showing the thermal decomposition of the secondary hydroxy groups. Absorption bands of amines and aromatics decreased in intensity and some of them shifted in wavenumbers, indicating the thermal decomposition of the epoxy matrix, but they did not disappear completely, indicating that some of the amines were left in the residue and polyaromatisation occurred [23]. The C═O (1742 cm^{-1} in DOPI and DOPP) and C—N (1696 cm^{-1} in DOPI) bands of the aliphatic ground bodies of the flame retardants decreased with increasing temperature, finally disappearing completely to reveal that the ground bodies of the flame retardants decomposed. Phosphorus bands (1475, 1118, 911 cm^{-1}) remained in the condensed phase during thermal decomposition, with some new P-bands at 1432 cm^{-1} (P—C_{Ar} stretching) and 1235 cm^{-1} (P═O stretching) observed at the end of thermal decomposition. Two additional absorption bands at 1207 and 1053 cm^{-1} were observed. They were attributed to P—N stretching vibrations [24], indicating a chemical reaction between phosphorus and the nitrogen of partially decomposed epoxy structures. These cross-linking reactions probably promote char formation. This is in agreement with the strongly enhanced residue of RTM6 + DOPP and RTM6 + DOPI compared to RTM6.

3.5. Pyrolysis: proposed decomposition pathway

On the basis of the results obtained for mass loss, evolved gas analysis and condensed product analysis,

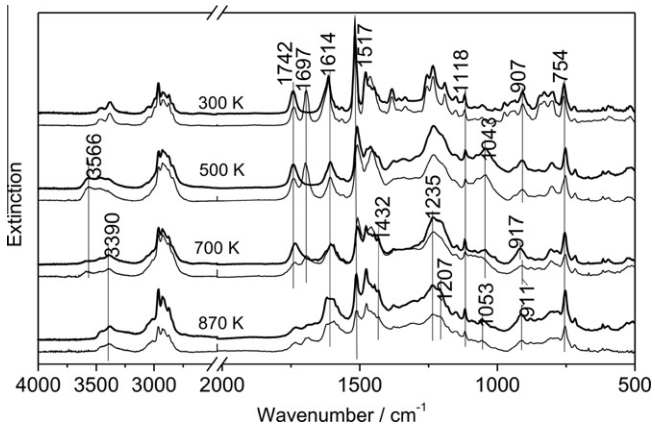

Fig. 4. Transmission FTIR spectra of the condensed phases of RTM6 + DOPP (thick solid line) and RTM6 + DOPI (thin solid line) at different stages of decomposition (300, 500, 700 and 870 K) at a heating rate of 10 K min^{-1} under nitrogen.

decomposition pathways were proposed for RTM6 + DOPP and RTM6 + DOPI. Fig. 5a shows the early stage of decomposition of RTM6. The decomposition starts with two competing mechanisms occurring on the 2-hydroxymethylene groups of the epoxy resin. On the one hand, dehydratisation takes place, indicated by the release of water. On the other hand, the scissoring of carbonyl derivatives out of the 2-hydroxymethylene groups yields secondary anilines, some of which are released in the subsequent gas phase. This pathway is not favoured for the thermal decomposition of RTM6 + DOPI since such a low amount of carbonyls was found in evolved gas analysis. The decomposition of the secondary hydroxy group is followed by the release of primary aniline derivatives and the formation of linear or cyclic unsaturated aromatic amines in the residue [21,25–27].

Since the ester group in the ground body of the two flame retardants is highly susceptible to hydrolysis (Fig. 5b), this is the first group of the flame retardants to decompose. A carbonylic acid functionality with the DOPO moiety is formed at the end of the chain, and a hydroxy group with the pentaerythritol or isocyanurate rest. In DOPI the nucleophilic hydroxy group attacks the carbonyl carbon of the isocyanurate ring and subsequently oxazolidinones are formed, observed in the evolved gas analysis next to isocyanuric acid, a further decomposition product of the ring. The carbonylic acid function still carrying the DOPO moiety decomposes either by decarboxylation and release of DOPO still bearing an ethylene group, or by splitting off acrylic acid and releasing DOPO. Part of the phosphorus is released in the gas phase and part remains in the residue, since interactions between the flame retardant and the epoxy matrix in the condensed phase were monitored in mass loss and condensed product analysis.

In Fig. 5c the reaction mechanism between the phosphorus and amino groups of the partly decomposed epoxy matrix is proposed. During this reaction P—N bonds are formed, which were observed in the infrared spectra of the residue. Since P—O—C_{Ar} absorption bands were observed in the residue, further reactions of DOPO moieties with aromatic structures from the epoxy matrix are reasonable.

4. Fire behaviour

4.1. Fire behaviour: flammability and forced-flaming behaviour

Table 4 summarises flammability results (reaction to a small flame) and cone calorimeter data.

RTM6 showed self-extinguishing in UL 94 with a classification of HB due to burning dripping and long burning times. The LOI was 25%. The addition of carbon fibres to RTM6 resulted in a strongly enhanced LOI value (+8.2%), but even though the CF suppressed burning dripping, the UL 94 remained HB due to long burning times. All the flame-retarded samples with and without CF showed an improvement in UL 94 between V-1 and V-0. The LOI of RTM6 with flame retardant was improved by around 12% for RTM + DOPP and by 9% for RTM6 + DOPI. The flame-retarded composites showed an amelioration of the LOI of +12% for RTM6-CF + DOPP and + 14% for RTM6-CF + DOPI in comparison to RTM6-CF. This points to a superposition of the increase in LOI due to the CF and the flame retardant in RTM6-CF + DOPP and a synergism for RTM6-CF + DOPI.

The ignitability of RTM6 + DOPP and RTM6 + DOPI did not change in comparison to RTM6. The time to ignition (t_{ig}) in the cone calorimeter did not change significantly. For the composites the addition of CF increased the t_{ig} by between 16 and 24 s in comparison to their non-reinforced equivalents. This is due in particular to the replacement of around 70 wt.% combustible material by CF. As other carbon materials, CF are inert in anaerobe pyrolysis conditions typical for most of the fire phenomena [28]. What is more heat absorption and emission behaviour of the black surface of the samples; the heat conductivity and heat capacity of the composites are changed by adding such a large amount of fibres crucially [3,29,30].

The heat release rate (HRR) of all materials is shown in Fig. 6a using an irradiance of 50 kW m^{-2}. After ignition RTM6, RTM6 + DOPP and RTM6 + DOPI showed a rapid increase in HRR with an intensive peak at the end of the burning. RTM6 + DOPP and RTM6 + DOPI showed a distinctive shoulder prior to the PHRR. RTM6-CF, RTM6-CF + DOPP, and RTM6-CF + DOPI showed a HRR curve com-

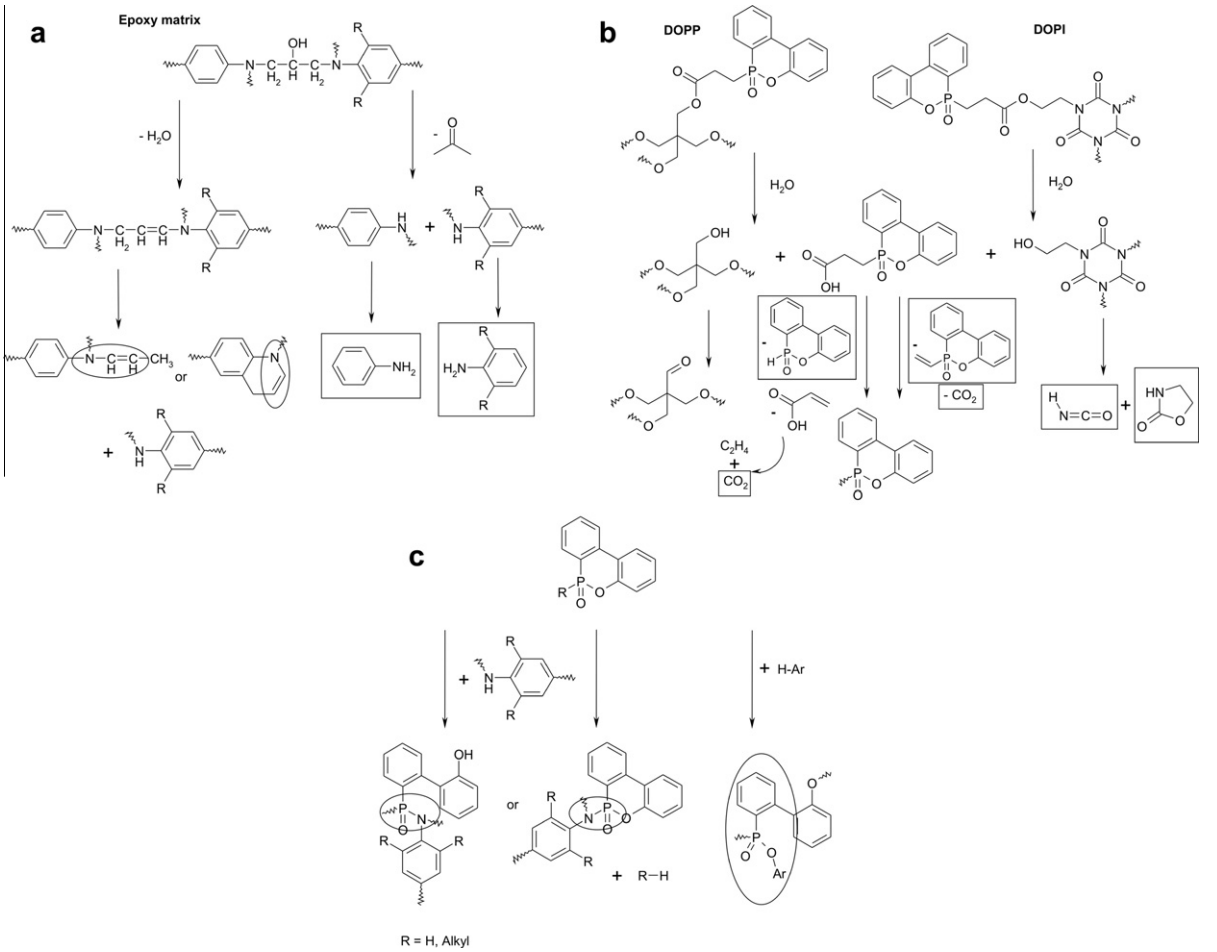

Fig. 5. Proposed thermal decomposition pathways of (a) RTM6, (b) DOPP and DOPI and (c) proposed interactions of decomposition products (square boxes = proven gaseous decomposition products, circles = proven structures in the solid residue, zigzag lines = cross-linking to other carbon or hydrogen atoms).

Table 4
Flammability results and cone calorimeter data of RTM6, RTM6-CF, RTM6 + DOPP, RTM6-CF + DOPP, RTM6 + DOPI and RTM6-CF + DOPI at an external heat flux of 50 kW m^{-2} (t_{ig} = time to ignition, PHRR = peak heat release rate, THE = total heat evolved, THE/ML = effective heat of combustion of the volatiles). The values are averaged from two measurements.

	RTM6	RTM6-CF	RTM6 + DOPP	RTM6-CF + DOPP	RTM6 + DOPI	RTM6-CF + DOPI
Flammability						
UL 94	HB	HB	V-1	V-0	V-0	V-0
LOI/% ± 1	25.0	33.2	37.9	45.3	34.2	47.7
Cone calorimeter at 50 kW m^{-2}						
t_{ig}/s ± 3	35	51	40	56	36	60
PHRR/kW m^{-2} ± 80	1719	347	1191	248	869	247
THE/MJ m^{-2} ± 3.0	74.2	26.2	44.8	19.9	41.5	20.0
Residue/wt.% ± 1.1	6.5	72.8	17.2	72.0	15.8	71.6
THE/ML/MJ $m^{-2}g^{-1}$ ± 0.1	2.4	2.2	1.5	1.6	1.4	1.5
TSR/m^2 m^{-2} ± 300	2725	1357	3848	2007	4026	1889
TCOR/g ± 0.15	2.32	0.59	3.20	1.32	3.39	1.35
PHRR/t_{ig}/kW $m^{-2}s^{-1}$	49.9	6.9	29.8	4.4	24.1	4.1

parable to charring materials, with only a slight PHRR and a long, drawn-out decrease in HRR up to the end of the burning.

The peak heat release rate (PHRR) and the total heat evolved (THE = total heat release at the end of burning) were strongly influenced by the addition of flame retardant

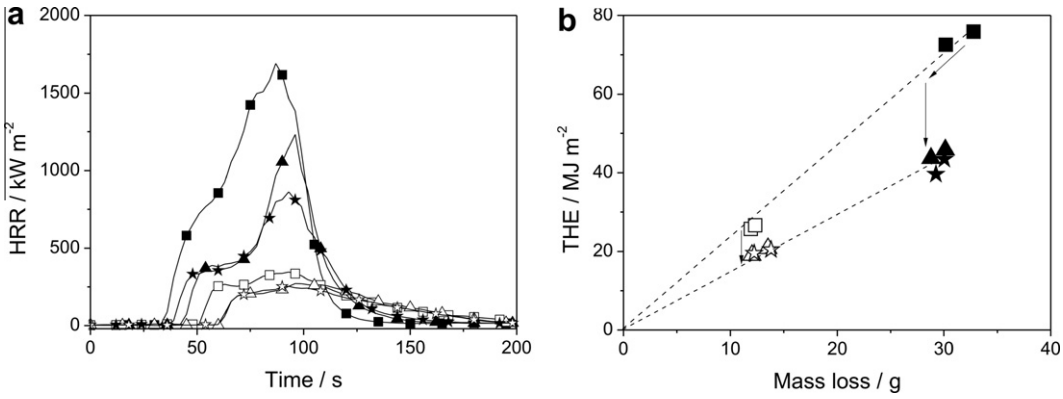

Fig. 6. (a) Heat release rate (HRR) and (b) gas-phase and condensed-phase action of RTM6 (filled squares), RTM6-CF (open squares), RTM6 + DOPP (filled triangles), RTM6-CF + DOPP (open triangles), RTM6 + DOPI (filled stars) and RTM6-CF + DOPI (open stars) at an external heat flux of 50 kW m^{-2}.

or CF or both compared to RTM6. The PHRR of the non-reinforced materials was highest for RTM6 and decreased in the order: RTM6 > RTM6 + DOPP > RTM6 + DOPI. The THE decreased considerably in the order RTM6 > RTM6 + DOPP > RTM6 + DOPI. The reduction of PHRR and THE in RTM6 + DOPP and RTM6 + DOPI indicates a strong flame-retarding action of DOPP and DOPI, respectively. Since the composites contain less than one third of combustible material, the PHRR and the THE were lowered significantly in all of the CF-composites investigated. Both flame retardants reduced the PHRR and THE in the order RTM6-CF > RTM6-CF + DOPP = RTM6-CF + DOPI, indicating a flame-retarding action in the composites as well.

The residue of RTM6 + DOPP and RTM6 + DOPI was increased in comparison to that of RTM6. This led to the shoulder in the HRR curve of RTM6 + DOPP and RTM6 + DOPI. The higher residue is in agreement with thermogravimetry results and confirms the condensed-phase mechanism of the flame retardants. The difference in residue of the composites is rather small. Subtracting the weight of the CF from the residue yields similar amounts of residue for all composites; hence the CF suppresses charring. This has already been reported in the literature [31,32].

A reduction in the effective heat of combustion of the volatiles, which is the THE per total mass loss (THE/ML), indicates gas-phase activity by the flame retardants. The lower the THE/ML in comparison to the non-flame-retarded material, the stronger the flame inhibition of the flame retardant. Furthermore flame inhibition goes along with incomplete combustion, which increases the smoke and the CO release in the gas phase. RTM6 + DOPP and RTM6 + DOPI strongly decreased the THE/ML by around 38–42% in comparison to RTM6. The total smoke release (TSR) and the total CO release (TCOR) were strongly increased. The flame inhibition corresponds with the phosphorus release in the gas phase shown in the pyrolysis. In the composites, the THE/ML is decreased by flame inhibition by around the same magnitude as for the thermosets, and the TSR and TCOR were increased in comparison to RTM6-CF.

Fig. 6b summarises the flame-retarding mechanisms of the thermosets and composites. The THE is plotted against the mass loss. For RTM6 flame-retarded with DOPP and DOPI, the THE is reduced due to gas-phase activity, indicated by a reduced slope, and condensed-phase activity, indicated by a decreased mass loss. However, the main flame-retarding mechanism for RTM6 + DOPP and RTM6 + DOPI is the action in the gas phase, since this mainly contributes to the reduction of the THE. In the composites only gas-phase activity occurs; therefore the slope is reduced but not the mass loss.

5. Conclusion

Oligomeric star-shaped flame retardants containing DOPO (DOPP and DOPI) were proposed for RTM6 and RTM6-CF. The glass transition temperatures of all materials and the mechanical properties, such as apparent ILSS and the critical strain energy release rate (G_{Ic}, G_{IIc}) were determined for the composites. Pyrolysis and fire behaviour were studied. Furthermore the influence on the fire behaviour exerted by high weight fractions of incorporated CF (~70%) was examined. The mass loss, the evolved gases and the condensed phase were analysed and decomposition models of the materials were developed.

The replacement of epoxy resin with DOPP led to an acceptable decrease in glass transition temperature while the replacement of epoxy resin with DOPI was at the acceptable limits. The reduction of the T_g is attributed to the reduction of the effective cross-linking points per volume. The mechanical behaviour of the composites in terms of ILSS, G_{Ic} and G_{IIc} was not affected significantly. Both flame retardants worked in the gas phase and in the condensed phase of RTM6. In the gas phase they worked via flame inhibition, indicated by phosphorus release detected in the evolved gases. Condensed-phase analysis showed that part of the phosphorus was incorporated into the char network by reactions of the phosphorus with partly decomposed RTM6. The char formation was increased.

The PHRR divided by the t_{ig}, (PHRR/t_{ig}), which is a measure for the flame spread, and the THE, which indicates the fire load, were decreased significantly due to flame inhibition and char formation in RTM6 + DOPP and RTM6 + DOPI, whereby flame inhibition was indentified as the main flame-retarding mechanism. The LOI was strongly

enhanced and the UL 94 resulted in V-1 and V-0 classification, respectively. The addition of CF to RTM6 + DOPP and RTM6 + DOPI decreased the fire risk in terms of flame spread and fire load even more than the flame retardants alone. Further, in the LOI a superposition for RTM6-CF + DOPP and a synergism for RTM6-CF + DOPI were found. The UL 94 resulted in V-0 for both materials. Adding CF alone did not ameliorate the UL 94. The UL 94 strongly demands flame-retarding effects, while the LOI was enhanced by simple replacement of 70 wt.% of combustible material by inert CF. However, an important difference between the thermosets and the composites is that the CF suppressed the charring. Therefore the flame retardants acted only via flame inhibition in the composites. The structures of the flame retardants did not influence the thermal decomposition significantly. Decomposition mechanisms were similar for both flame retardants.

Acknowledgement

The authors thank the German Research Foundation (DFG) for its financial support (DFG SCHA 730/10-1, DFG DO 453/6-1, DFG AL 474/14-1).

References

[1] Lee H, Neville K. Handbook of epoxy resins. New York: McGraw-Hill; 1982.
[2] Ellis B. Chemistry and technology of epoxy resins. London, New York: Blackie Academic and Professional; 1993.
[3] Mouritz AP, Gibson AG. Fire properties of polymer composite materials. Dordrecht: Springer; 2006.
[4] Weil ED, Levchik SV. A review of current flame retardant systems for epoxy resins. J Fire Sci 2004;22(1):25–40.
[5] Levchik SV, Weil ED. A review of recent progress in phosphorus-based flame retardants. J Fire Sci 2006;24(5):345–64.
[6] Hergenrother PM, Thompson CM, Smith JJG, Connell JW, Hinkley JA, Lyon RE, et al. Flame retardant aircraft epoxy resins containing phosphorus. Polymer 2005;46(14):5012–24.
[7] Artner J, Ciesielski M, Walter O, Döring M, Perez RM, Sandler JKW, et al. A novel DOPO-based diamine as hardener and flame retardant for epoxy resin systems. Macromol Mater Eng 2008;293(6):503–14.
[8] Liu YL. Epoxy resins from novel monomers with a bis-(9,10-dihydro-9-oxa-10-oxide-10-phosphaphenanthrene-10-yl-) substituent. J Polym Sci Part A Polym Chem 2002;40(3):359–68.
[9] Perez R, Sandler J, Altstädt V, Hoffmann T, Pospiech D, Ciesielski M, et al. Effect of DOP-based compounds on fire retardancy, thermal stability, and mechanical properties of DGEBA cured with 4,4′-DDS. J Mater Sci 2006;41(2):341–53.
[10] Schartel B, Balabanovich AI, Braun U, Knoll U, Artner J, Ciesielski M, et al. Pyrolysis of epoxy resins and fire behavior of epoxy resin composites flame-retarded with 9,10-dihydro-9-oxa-10-phosphaphenanthrene-10-oxide additives. J Appl Polym Sci 2007;104(4):2260–9.
[11] Perez R, Sandler J, Altstädt V, Hoffmann T, Pospiech D, Ciesielski M, et al. Effective halogen-free flame retardants for carbon fibre-reinforced epoxy composites. J Mater Sci 2006;41(15):4981–4.
[12] Wang CS, Lin CH. Properties and curing kinetic of diglycidyl ether of bisphenol A cured with a phosphorus-containing diamine. J Appl Polym Sci 1999;74(7):1635–45.
[13] Lin CH, Cai SX, Lin CH. Journal of polymer science part a: flame-retardant epoxy resins with high glass-transition temperatures. II. Using a novel hexafunctional curing agent: 9, 10-dihydro-9-oxa-10-phosphaphenanthrene 10-yl-tris(4-aminophenyl) methane. Polym Chem 2005;43(23):5971–86.
[14] Perez R, Sandler J, Altstädt V, Hoffmann T, Pospiech D, Artner J, et al. Effective halogen-free flame retardancy for a monocomponent polyfunctional epoxy using an oligomeric organophosphorus compound. J Mater Sci 2006;41(24):8347–51.
[15] Schartel B, Braun U, Balabanovich AI, Artner J, Ciesielski M, Döring M, et al. Pyrolysis and fire behaviour of epoxy systems containing a novel 9,10-dihydro-9-oxa-10-phosphaphenanthrene-10-oxide-(DOPO)-based diamino hardener. Europ Polym J 2008;44(3):704–15.
[16] Ciesielski M, Schäfer A, Döring M. Novel efficient DOPO-based flame-retardants for PWB relevant epoxy resins with high glass transition temperatures. Polym Adv Techn 2008;19(6):507–15.
[17] Perret B, Schartel B, Stöß K, Ciesielski M, Diederichs J, Döring M, et al. A new halogen-free flame retardant based on 9,10-dihydro-9-oxa-10-phosphaphenanthrene-10-oxide for epoxy resins and their Carbon fiber composites for the automotive and aviation industries. Macromol Mater Eng 2011;296(1):14–30.
[18] Krämer J, Beier U, Altstädt V, Stöß K, Diederichs J, Ciesielski M, Döring M, Perret B, Schartel B. New halogen free flame retardants for high performance epoxy resins. SAMPE fall technical conference proceedings: advanced materials and processes: enabling the future, October 11–14, 2010, Salt Lake City, Utah. Society for the Advancement of Material and Process Engineering, CD-ROM, 2010; accepted.
[19] Barbero EJ. In: introduction to composite materials design. Philadelphia: Taylor and Francis; 1999.
[20] Bishop DP, Smith DA. Combined pyrolysis and radiochemical gas chromatography for studying the thermal degradation of epoxy resins and polyimides. I. The degradation of epoxy resins in nitrogen between 400 and 700 °C. J Appl Polym Sci 1970;14(1):205–23.
[21] Lee L-H. Mechanisms of thermal degradation of phenolic condensation polymers. II. Thermal stability and degradation schemes of epoxy resins. J Polym Sci Part A General Papers 1965;3(3):859–82.
[22] Levchik SV, Camino G, Luda MP, Costa L, Costes B, Henry Y, et al. Mechanistic study of thermal behavior and combustion performance of epoxy resins: I homopolymerized TGDDM. Polym Adv Technol 1995;6(2):53–62.
[23] Factor A. Fire and polymers hazards identification and prevention. ACS symposium series, vol. 425. Washington: ACS; 1990:274–287.
[24] Thomas LC. Interpretation of the infrared spectra of oganophosphorus compounds. London, New York, Rheine: Heyden and Son Ltd.; 1974.
[25] Lee L-H. Mechanisms of thermal degradation of phenolic condensation polymers. III. Cleavage of phenolic segments during the thermal degradation of uncured epoxy resins. J Appl Polym Sci 1965;9(5):1981–9.
[26] Paterson-Jones JC, Percy VA, Giles RGF, Stephen AM. The thermal degradation of model compounds of amine-cured epoxide resins. II. The thermal degradation of 1,3-diphenoxypropan-2-ol and 1,3-diphenoxypropene. J Appl Polym Sci 1973;17(6):1877–87.
[27] Levchik SV, Weil ED. Thermal decomposition, combustion and flame-retardancy of epoxy resins – a review of the recent literature. Polym Int 2004;53(12):1901–29.
[28] Lyon RE. In: Harper CA, editor. Handbook of building materials for fire protection. New York: McGraw-Hill; 2004. [chapter 3:3.1–3.51].
[29] Hohenberger W. In: Zweifel H, editor. Plastics additives handbook. Munich: Hanser; 2001. pp. 901–943.
[30] Kashiwagi T, Grulke E, Hilding J, Groth K, Harris R, Butler K, et al. Thermal and flammability properties of polypropylene/carbon nanotube nanocomposites. Polymer 2004;45(12):4227–39.
[31] Levchik SV, Camino G, Costa L, Luda MP. Mechanistic study of thermal behaviour and combustion performance of carbon fibre-epoxy resin composites fire retarded with a phosphorus-based curing system. Polym Degrad Stab 1996;54(2–3):317–22.
[32] Braun U, Balabanovich AI, Schartel B, Knoll U, Artner J, Ciesielski M, et al. Influence of the oxidation state of phosphorus on the decomposition and fire behaviour of flame-retarded epoxy resin composites. Polymer 2006;47(26):8495–508.